Polymer Degradation and Stability 98 (2013) 1006–1014

Contents lists available at SciVerse ScienceDirect

Polymer Degradation and Stability

journal homepage: www.elsevier.com/locate/polydegstab

Effect of PLA grades and morphologies on hydrolytic degradation at composting temperature: Assessment of structural modification and kinetic parameters

Giuliana Gorrasi, Roberto Pantani*

Dept. of Industrial Engineering, University of Salerno, Via Ponte Don Melillo, I-84084 Fisciano (SA), Italy

ARTICLE INFO

Article history:
Received 26 November 2012
Received in revised form
30 January 2013
Accepted 10 February 2013
Available online 19 February 2013

Keywords:
PLA
Hydrolysis
Autocatalytic mechanism
Degradation

ABSTRACT

The present work focuses on a study of the hydrolysis process of different commercial grades of polylactic acid (PLA). The aim was to evaluate the fundamental factors affecting hydrolysis in aqueous medium at 58 °C, namely the temperature indicated by the international standards for biodegradation during composting, and the kinetic constant of the reaction involved in such process. We analyzed samples of PLA with different D-isomer content, having amorphous and semi-crystalline structures. The hydrolysis process was followed, as function of the time, by means of different techniques: pH variation, variation of weight (%) of samples, crystallinity degree using DSC analysis, FTIR and WAXD investigation, molecular weights and molecular weight distribution by GPC analysis. The experimental data were used to describe the kinetic of hydrolysis phenomenon, assuming an autocatalytic mechanism.

1. Introduction

Poly(lactic acid) (PLA) is a biodegradable polymer, with several applications in biomedical and pharmaceutical fields as a material used in surgical operations, tissue regeneration, and drug delivery systems [1]. PLA has also been attracting much interest as a valid alternative to commercial oil-derived polymers such as polyethylene, polypropylene, poly(ethylene terephthalate) and polystyrene, because of its renewable resources origin Ref. [2], and for feedstock recycling into L-lactic acid by hydrolysis [3,4] or into L, L-lactide by pyrolysis [5,6]. Many studies, in looking to control the hydrolysis of polymeric implant devices in-vivo, have reported on the hydrolytic degradation of aliphatic polyesters, including PLA, analyzing the factors which can influence such phenomenon [7–14]. Generally, it has been recognized that the polyesters undergo an auto-catalytic random chain scission during hydrolysis as a result of acceleration by their carboxyl end groups [15–20]. For both biomedical and consumer applications, it is of major importance to understand the degradation characteristics of PLA. It is well known that the degradation products of PLA are known to reduce local pH, accelerate degradation and induce inflammatory reactions [21]. The degree of erosion associated with the biodegradation process is usually estimated from measurements of mass loss. The erosion process can be described by phenomenological diffusion–reaction mechanisms. An aqueous medium diffuses into the polymeric material while oligomeric products diffuse outwards. Within the polymeric matrix, hydrolytic reactions take place, mediated by water and/or enzymes. For most biodegradable materials, especially synthetic polymers like PLA, biodegradation is considered to consist in a sequential mechanism in which the first step is the hydrolysis which reduces the molecular weight, and the second step is the assimilation by the microorganisms [22]. For this reason it is of fundamental importance the knowledge of this phenomenon and the correlation either with the chain microstructure or the morphology of manufacture, because water is the most interactive molecule of PLA after its lifecycle. Polymer degradation is the first step of the erosion phenomenon and can be estimated by measuring the molecular weight decrease. During this first phase, aqueous solution penetrates the polymer, followed by hydrolytic degradation, converting this very long polymer chain into shorter water-soluble fragments, which can be regarded as a reverse polycondensation process; for PLA it has been found that it becomes soluble in water for molecular weight, Mn, below ≈20,000 (g/mol) [13]. In this paper we analyzed the hydrolytic behavior of different PLA grades submitted to different thermal treatments in bidistilled water. The aim was to correlate structural and morphological parameters to the hydrolytic phenomenon. The kinetic of hydrolysis was, then, described for the different samples hypothesizing an auto-catalytic random hydrolysis as the main reaction mechanism [23–25]. Most of literature studies are

* Corresponding author. Tel.: +39 089964141.
E-mail address: rpantani@unisa.it (R. Pantani).

0141-3910/$ – see front matter © 2013 Elsevier Ltd. All rights reserved.
http://dx.doi.org/10.1016/j.polymdegradstab.2013.02.005

conducted at 37 °C and buffer solutions, because are finalized at controlled release or at in-vivo dissolution. In this work we conducted the hydrolysis tests at 58 °C, namely at the temperature at which biodegradation tests are carried out, so that a detailed monitoring of pH is essential during the hydrolysis processing. In addition, the hydrolysis phenomenon results faster at 58 °C, compared to 37 °C, and easy to be followed in a reasonable range of time [12,26,27]. The chosen temperature is also slightly above the Tg of the material, so that it is possible to analyze morphological transformation hydrolysis inducted. It is worth underlying that the choice of analyzing semicrystalline samples was dictated by the fact it is generally considered that the crystalline regions hydrolyze much more slowly than the amorphous regions, however the works which analyze this aspect are rare in the literature. This results in the fact that it is still not clear how and in which way the crystalline domains of PLA are influenced by the hydrolysis process.

2. Experimental

2.1. Materials

Three commercial grades of PLA were adopted in this work. They were produced by Natureworks with the commercial names of 4060D, 2002D and 4032D. The average molecular weight (Mw) of all three grades is in the range 190–230 KDa, whereas the polydispersity index was about in the range 1.7–1.9. The main difference among the three grades is the D-lactide content which is about 12% for 4060D, about 4% for 2002D and about 2% for 4032D. The amount of D-lactide deeply influences the crystallinity of polylactides: on increasing the D-lactide percentage, the crystallization kinetics becomes slower and the maximum attainable crystalline content reduces. As a consequence, the 4060D grade is amorphous, the 2002D is semicrystalline, with a maximum crystallinity degree of about 35% [28,29], the 4032D is semicrystalline, with a maximum crystallinity degree of about 45%. The relevant properties of the materials adopted are summarized in Table 1.

2.2. Methods

The pellets of each of the materials were dried for 24 h under vacuum at a temperature of 60 °C. They were then compression molded in the shape of films having a thickness of 150 μ. The temperature for compression molding was 200 °C, the time was 15 min. The samples were then cooled down in air.

Only for the material 4032D, some films obtained were placed in a oven at 110 °C for 5 h. These samples will be referred to as "crystalline 4032D".

Hydrolysis tests were conducted in bidistilled water at 58 °C whose pH was measured to be 5.7. This temperature was selected because it is the temperature adopted for biodegradation tests according to ASTM and ISO standards. Several films (having a thickness of about 150 μ, and weighing about 50 mg) of each of the samples were placed each in one glass vessel containing water. The mass amount of water was fixed in the ratio 500:1 with the mass of the dry sample. Every 24 h each vessel was emptied by sucking the liquid by a syringe with a needle having a diameter of 0.2 mm. The pH of the liquid was measured by a Crison pH-meter at 25 °C calibrated daily. Fresh bidistilled water, in the same amount taken out, was then added to the vessel containing the sample and the vessel was put again in water at 58 °C. At selected days of hydrolysis, the vessels containing the samples were emptied by sucking the liquid by the syringe, dried under vacuum at 60 °C for 2.5 h and weighed. The weight of the sample was then obtained by subtracting the tare. The whole operation lasted less than 3 h. One of the films of each sample, after the weighing operation, was placed in a desiccator for further analysis (X-Rays, DSC, GPC, FTIR). All the others vessels were refilled with water in the selected 500:1 ratio and put again in water at 58 °C. It is worth mentioning that the adopted procedure requires that pH and weight loss data are collected on several (from 3 to 7) samples at the same hydrolysis time. The reproducibility of the data was found to be within 10% for pH data and 5% for weight loss data.

X-ray diffraction measurements (XRD) were performed with a Brucker diffractometer (equipped with a continuous scan attachment and a proportional counter) with Ni-filtered Cu Kα radiation ($\lambda = 1.54050$ Å).

Differential scanning calorimetry (DSC) analysis of the samples was carried out on samples with a mass of about 4 mg. The tests were carried out by means of a DTA Mettler Toledo (DSC 822) under nitrogen atmosphere. The samples were heated from −10 °C to 200 °C at 10 °C/min.

X-ray diffraction measurements (XRD) were performed with a Brucker diffractometer (equipped with a continuous scan attachment and a proportional counter) with Ni-filtered Cu Kα radiation ($\lambda = 1.54050$ Å).

IR spectra were collected in transmission mode by means of Midac spectrometer in the mid-infrared range (400–4000 cm^{-1}).

The measurements of molecular weight distribution were carried out by a Waters Breeze 2 HPLC system. The samples were dissolved in tetrahydrofuran (THF) at 58 °C and then the solution was filtered by means of a Chromafil PTFE 0.45 μm filter.

Table 1
Relevant properties of the materials adopted in this work.

Material	Mw [KDa][a]	PI[a]	D-lactide	Tg [°C][b]	Tm [°C][c]
4060D	188	1.8	12%	57	–
2002D	215	1.9	4%	59	150
4032D	200	1.8	1.5%	61	170

[a] Measured by GPC analysis on the as-received pellets.
[b] Measured during DSC heating ramp at 10 °C/min.
[c] Peak of the melting endotherm during DSC heating ramp at 10 °C/min.

3. Results and discussion

3.1. Weight loss

Fig. 1 reports weight loss (%) as function of time (days) for all the analyzed samples. PLA 4060D, having the largest D enantiomer content, shows the fastest rate in weight loss, and reaches the value of 70% after about 30 days. Samples with lower D enantiomer content, either amorphous or semicrystalline, show very similar and slower rates of weight loss. The 4032D crystallized from the solid presents however a slower weight loss at times longer than about 30 days, thus revealing a higher resistance to the hydrolytic phenomenon. An optical analysis of the samples is also shown in Fig. 1. It is clear from the pictures that the samples soon become fragile and loose integrity even without any mechanical contact (it is important to notice that with the procedure adopted the samples are never touched during the tests).

3.2. pH variation

The pH of the degradation medium was followed as function of time (days) and is reported in Fig. 2. As mentioned in the methods section, the pH of the water was measured to be 5.7 before getting into contact with the samples. Soon after the pH measurement, the degradation medium was replaced with pure water every day. It is evident from Fig. 2 that for the amorphous samples the pH of degradation medium increases initially and then decreases.

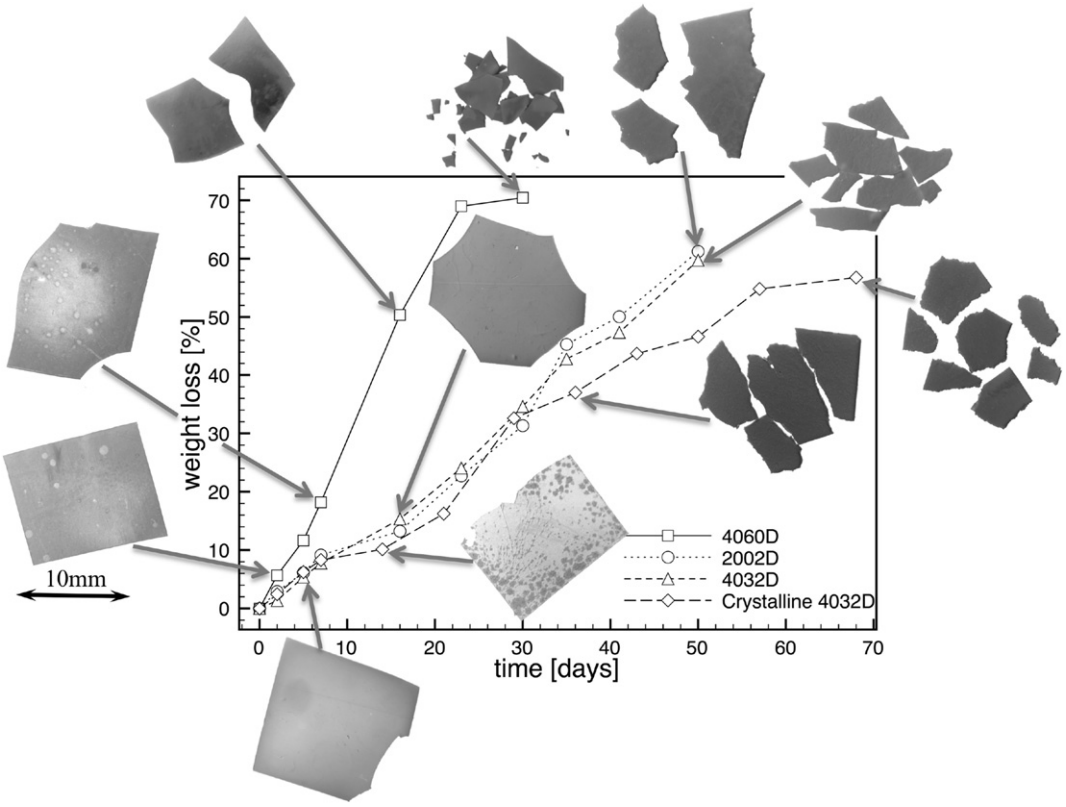

Fig. 1. Weight loss upon time for all the samples analyzed in this work. Optical images of the sample are also reported.

The duration of the period in which the degradation medium presents basicity is inversely proportional to the D enantiomer content. The degradation medium in which the crystalline PLA sample is placed does not reveal any increase of the pH but just a continuous reduction. After about 20 days of hydrolysis, pH values reach a plateau value which is independent either of the morphology or the D percentage. This plateau value, between 3 and 4, is coherent with pKa of PLA oligomer [30]. This value is still lower than the pH of the degradation medium which, as recalled above, was measured as 5.7. This means that the degradation continues up to the last monitored day. It is worth noticing that for 4060D sample, after reaching a minimum between 10 and 20 days, the pH starts to increase before reaching the common plateau value. This is a clue of a reduction in degradation rate.

It was observed that for biodegradable polymers water diffusion is normally very fast compared to water-mediated hydrolysis [31]. Therefore, water can be assumed, in many cases, to be uniformly distributed within the polymer from the beginning of erosion process, and hydrolysis promotes homogenous bulk erosion [18]. The polymeric ester groups can be easily hydrolyzed, leading to chain scission. Ester hydrolysis can be either acid or base catalyzed [32]. In Fig. 3 the acid based hydrolysis mechanism, most common in PLA degradation, is presented [31].

We can assume that the whole hydrolysis process can occur in three phases: i) diffusion of H_3O^+ into the polymeric bulk, that means excess of OH^- in solutions that justifies pH increasing, ii) hydrolysis reaction, iii) counter-diffusion of reaction products (i.e. carboxylic acids, alcohols, oligomers…).

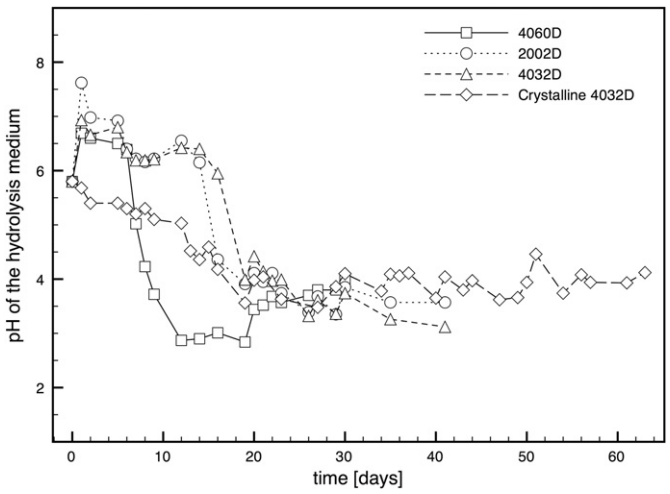

Fig. 2. Measurements of pH of the degrading medium upon time. The pH of the water adopted was measured to be 5.7 and the water was changed every day.

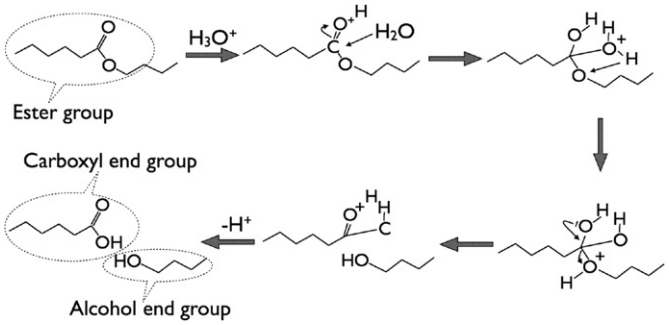

Fig. 3. Scheme of the acid based hydrolysis mechanism.

In the case of crystalline sample we do not observe a pH increase during the first days of water immersion, but a quite constant value of such parameter up to about 10 days, followed by a slow drop from 10th to 20th day of contact, and a plateau reached value. Nevertheless, during the first 30 days, the weight loss of this sample is the same of the other initially amorphous samples having similar D-lactide contents. This suggests that for crystalline morphology the step "i" of diffusion of H_3O^+ into the polymeric bulk, accompanied by excess of OH^- in solutions, is balanced by the step "iii" of counter-diffusion of reaction products, probably because of a predominance of surface hydrolysis.

3.3. Calorymetric analysis (DSC)

Some of the thermograms measured during the calorimetric heating ramps are reported in Fig. 4 as a function of hydrolysis time. As far as the 4060D sample (Fig. 4a) it can be evinced that the initially amorphous sample presents a clear endothermic peak already after 5 days of hydrolysis. This is a clear clue that, in spite of the fact that this material is unable to crystallize when cooled from the melt, some crystallinity can develop when it is immersed in water, even if at a temperature not far from the glass transition temperature, Tg. This can be due to both the mobility enhancement due to the plasticizing effect of water and the presence of smaller, faster crystallizing molecules resulting from the hydrolysis process. It is furthermore clear that the Tg reduces during time, as evident from the second heating scan (dotted lines in Fig. 4). This is clearly due to an enhanced mobility of the molecules, as a consequence of the hydrolysis process. The other two amorphous PLA grades (2002D in Fig. 4b and 4032D in Fig. 4c) present similar behavior. After 16 days, their crystallization kinetics is significantly enhanced, as demonstrated by the fact that they present a clear cold crystallization peak (not so evident at shorter times) at about 110 °C. The temperature of the melting peak decreases on increasing time and this phenomenon takes place either during the first (crystals formed during hydrolysis tests) and during the second heating ramp (crystals formed during heating in dry conditions). Also for 2002D and 4032D samples the Tg decreases during hydrolysis time. Concerning the crystalline 4032D sample, similar phenomena are observed. The melting peak temperature measured during the first heating scan decreases with time, revealing that the crystalline regions are also affected by the hydrolysis process. Furthermore, a clear difference in the melting peak temperature between the first and the second heating scans is present in this case.

A summary of DSC results is reported in Table 2

The morphology changes during hydrolysis appear clear on analyzing the WAXD spectra of the samples. Fig. 5 reports some amorphous spectra representative of the starting amorphous samples, and the crystalline one at different hydrolysis times. It can be noticed that the 4060D sample, initially showing only the amorphous halo, clearly presents crystalline peaks already after 5 days. The main 2θ peak at 16.5° in Fig. 5 was indexed as a (110)/(200) reflection of a-form homo-crystal structure [33], similar to those observed after degradation of low molecular weight PLA

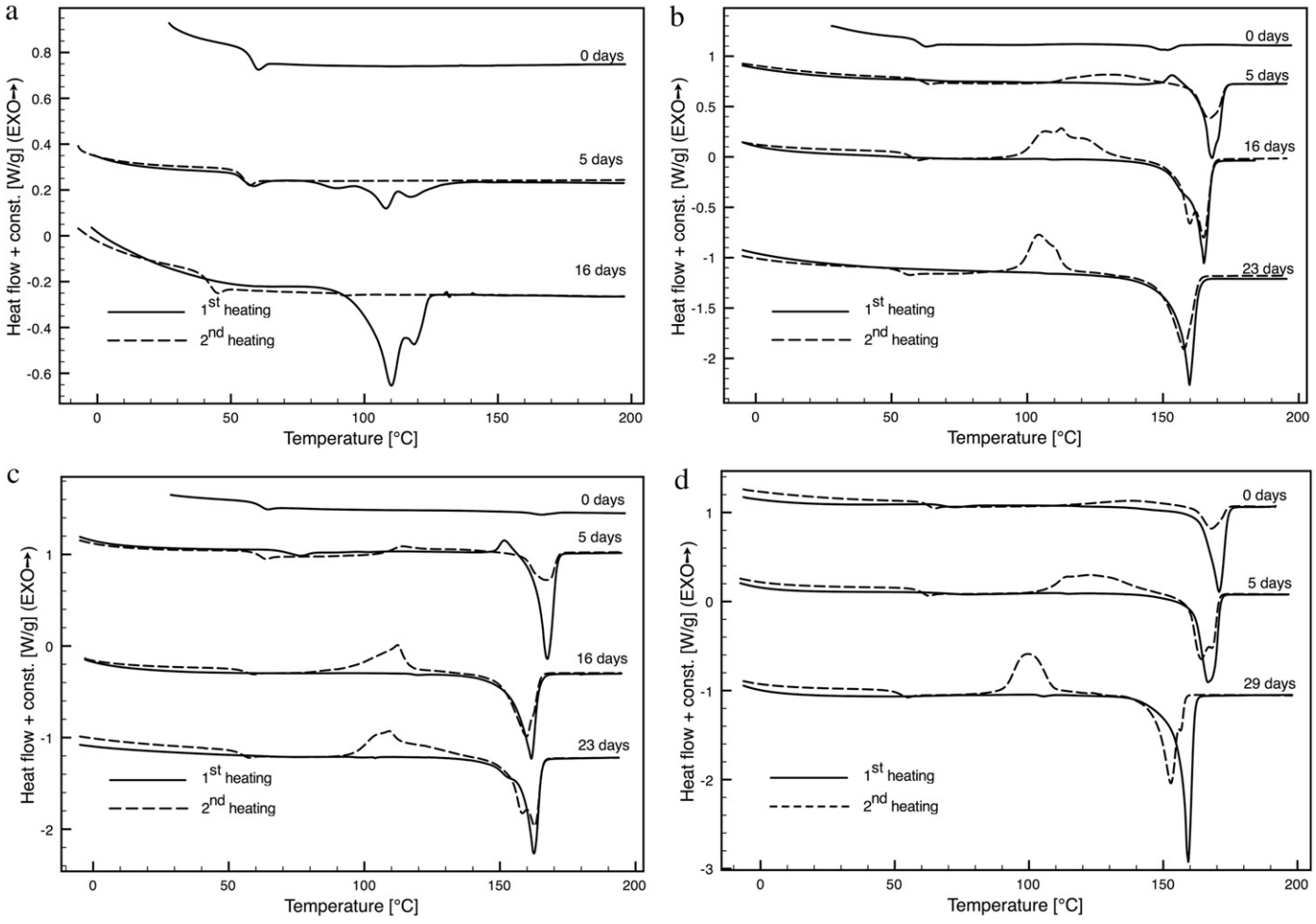

Fig. 4. DSC thermograms a) 4060D; b) 2002d; c) 4032D; d) crystalline 4032D sample, at selected times of hydrolysis.

Table 2
Summary of DSC results: Tg was measured during 2nd hating scan (at 10 °C/min), the reported Tm refers to the highest-temperature peak of the melting endotherm during 1st heating ramp (at 10 °C/min).

Sample		Days of hydrolysis				
		5	7	16	23	29
4060D	Tg [°C]	54.4	47.9	41.8		
	Tm [°C]	117.8	113.2	118		
2002D	Tg [°C]	61.5	59.5	56.5	53.4	
	Tm [°C]	167.7	168.5	165.1	159.6	
4032D	Tg [°C]	60.7	59.8	56.0	54.5	
	Tm [°C]	167.2	167.6	161.5	162.2	
Cryst 4032D	Tg [°C]	59.6	59.5		52	
	Tm [°C]	166.6	167.2			159.2

[8]. This stable α-form homo-crystal structure was also found as the major component in PLA residues after degradation, but some minor peaks were also observed over a broad range of 2θ values [13]. These minor reflections at 2θ = 12° and 22° were indexed as (100)/(010)/(−110) and (110)/(−120)/(−210) of stereo-complex crystals [33,34]. The degree of crystallinity increases on increasing the hydrolysis time. The starting crystalline sample (4032D), after long hydrolysis time (29 days) shows less perfection degree of crystalline domains, as evidenced by the widening of the main peak at 16.5° of 2θ. This is in agreement with DSC analysis, in which the melting temperature of crystalline 4032D sample, after 29 days of hydrolysis is about 15° lower than the starting film.

The increase of crystallinity during hydrolysis can also be assessed by FTIR [35]. Results obtained by the analysis of IR-spectra are reported in Fig. 6 for some of the samples analyzed. The reported spectra were obtained after subtracting a baseline from 810 to 955 cm^{-1} and after scaling in such way that the peak at 956.5 cm^{-1} presents the same height for all the samples. It can be noticed that the absorption band at 920 cm^{-1} (due to flexural C–H bond vibration), representative of the crystalline structure of PLA [36] increases with hydrolysis time for both the crystalline 4032D sample and the 4060D sample. For the latter one, the increase is more evident. Also the peak at 872 cm^{-1}, which is also assigned to of PLA crystals [37], increases with time, whereas the shoulder at about 862 cm^{-1} seems not to change with time suggesting that both peaks at 920 and at 862 cm^{-1} can be used as reference for estimating the crystallinity content.

The crystallinity degree was calculated from the thermograms measured during the first heating scan according to the formula

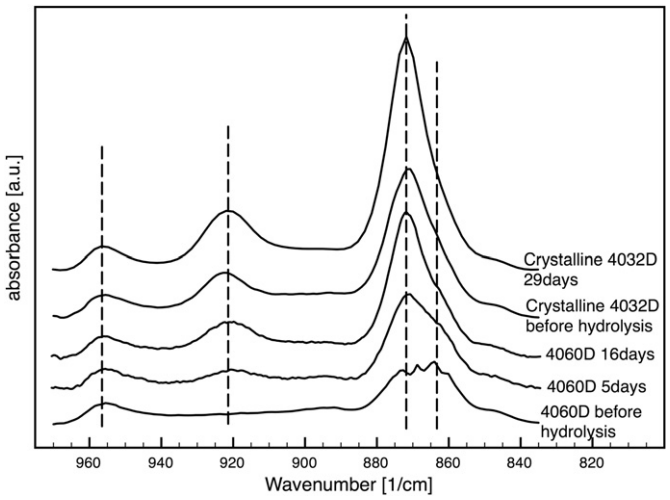

Fig. 6. FTIR spectra of 4060D and crystalline 4032D samples before and after selected times of hydrolysis.

$$\chi(t) = \int_0^t \frac{\delta Q}{\delta t} dt \Big/ \int_0^{t_\infty} \frac{\delta Q}{\delta t} dt = \frac{\Delta H(t)}{\Delta H_\infty} \quad (1)$$

in which $\delta Q/\delta t$ is the heat flow measured by the calorimeter, ΔH is the integral of the heat flow after the baseline subtraction, and ΔH_∞ is the latent heat of crystallization of a fully crystalline PLA, which can be found in the literature to be 93 J/g [38].

The results are reported in Fig. 7. It can be noticed that all the samples significantly increase their crystalline content during the hydrolysis tests. These crystallinity degrees are very high if compared with the maximum value reachable by the same materials as a consequence of thermal treatments (less than 45%). This can be partly due to the erosion of the amorphous portions, but is evidently due to a crystallization of the amorphous phase, since most of the samples were amorphous at the beginning of the test. Also the 4060D sample, which is unable to crystallize after thermal treatments, presents a significant degree of crystallinity after the first days of hydrolysis, when the weight loss is less than 10%.

The crystallinity degree can increase by effect of two possible phenomena: crystallization of the amorphous parts and erosion of the amorphous parts. Some insights about these phenomena can be obtained by coupling the data of crystallinity evolution and those of weight loss.

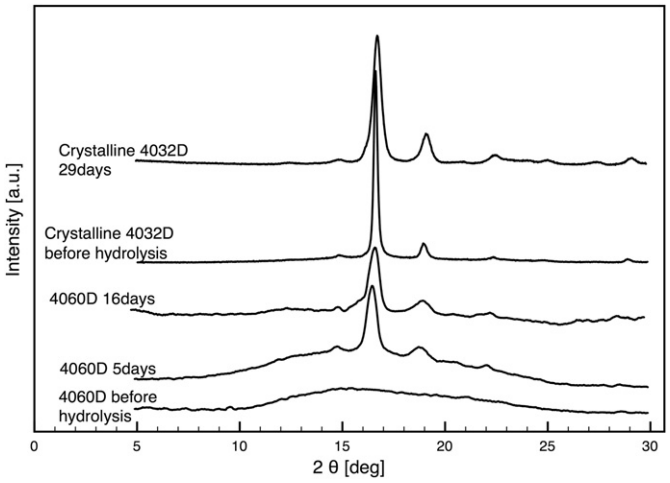

Fig. 5. WAXD spectra of 4060D and crystalline 4032D samples before and after selected times of hydrolysis.

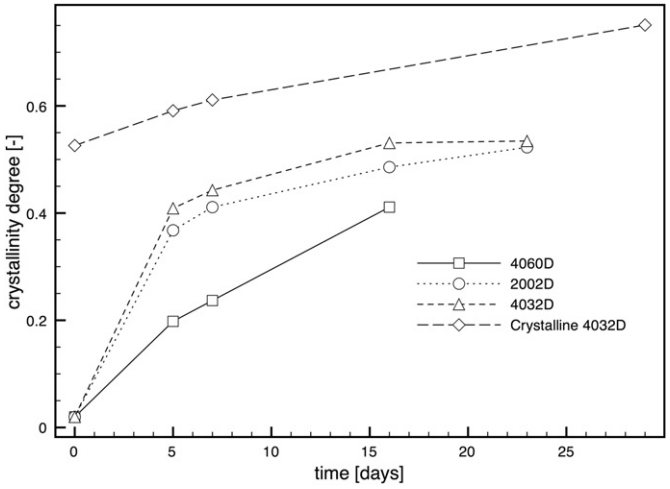

Fig. 7. Crystallinity degree measured from 1st heating calorimetric scans on the samples at selected times of hydrolysis.

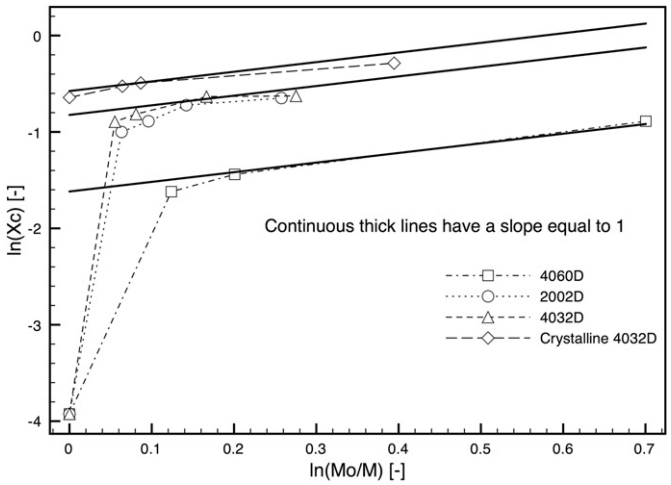

Fig. 8. Crystallinity evolution versus weight loss data during hydrolysis tests. The slope of the continuous lines is equal to 1.

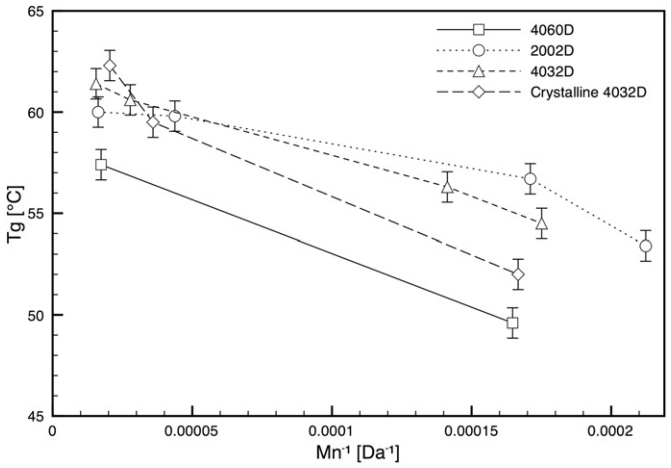

Fig. 10. Dependence of Tg (measured during the second heating scan) on the reciprocal of the number average molecular mass.

The crystallinity degree, *Xc*, can be defined as

$$Xc = \frac{Mc}{Mt} = \frac{Mc}{Mc + Ma} \tag{2}$$

where *Mt* is the mass of the sample, *Ma* and *Mc* are the masses of the amorphous and crystalline parts, respectively.

Assuming that *Mc* does not change during time (namely that no crystallization or hydrolysis of crystal portions occur), the time derivative of Eq. (2) results in the following Eq. (3)

$$\frac{1}{Xc}\frac{dXc}{dt} = -\frac{1}{Mt}\frac{dMt}{dt} \tag{3}$$

which can be also written as

$$\frac{d\ln(Xc)}{dt} = \frac{d\ln\left(\frac{Mo}{Mt}\right)}{dt} \tag{4}$$

in which *Mo* is the initial mass of the sample. Eq. (4) states that, if the mass of the crystal inside the sample does not change with time (namely if the crystallinity degree increases just by effect of the erosion of the amorphous portions) a plot reporting the logarithm of the crystallinity degree versus the logarithm of the reciprocal of the ratio *Mo*/*Mt* would present a slope equal to 1. A larger slope would indicate that the crystallinity degree increases also by effect of the crystallization of the amorphous parts; a smaller slope would mean that also crystalline portions are eroded.

In Fig. 8 the data of crystallinity evolution (reported in Fig. 6) and of weight loss (reported in Fig. 2) are combined in the form required by Eq. (4) and plotted for each of the samples analyzed in this work.

It can be noticed that at early times the slope is much larger than 1 (especially for initially amorphous samples), indicating that the samples do crystallize; at longer times the slope becomes equal to 1, indicating that the crystallinity degree increases by effect of the erosion of the amorphous parts. The latest points present a slope slightly smaller than 1, indicating that hydrolysis is attacking also the crystalline regions.

3.4. Gel permeation chromatography

Fig. 9 reports the Mw [Da] (a) and Mn [Da] (b) of all samples, as function of hydrolysis time (days).

As consequence of hydrolytic process, the polymeric chains undergo a breakdown with a decreasing of Mw [Da] and Mn [Da] and also PDI. PDI index shows small variation with hydrolysis time, so that the data reported Fig. 9 appear very similar for both parameters.

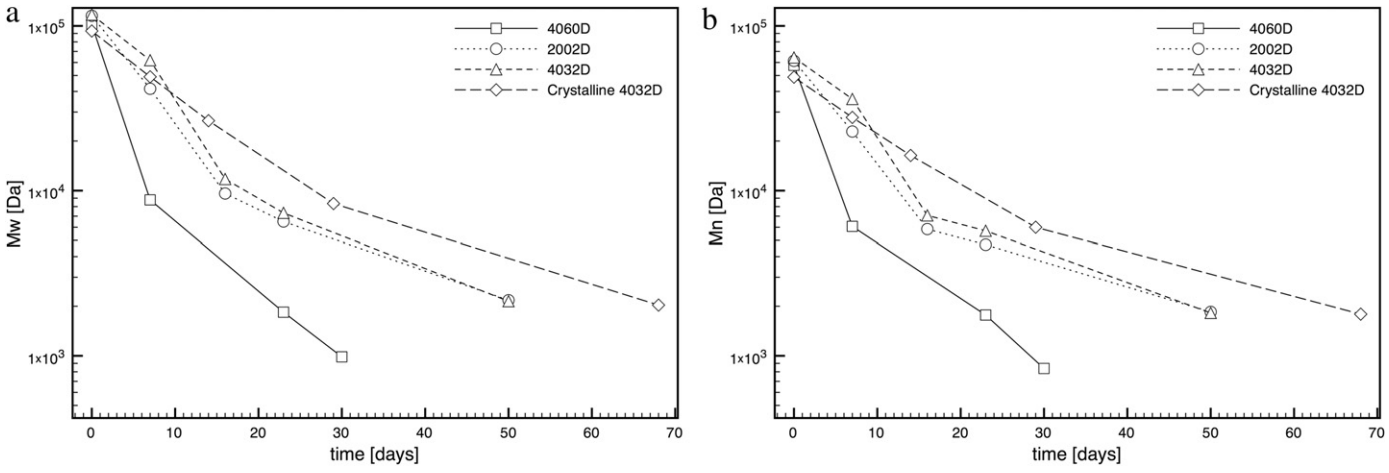

Fig. 9. Time dependence of a) weight average molecular mass, b) number average molecular mass, for all the samples analyzed in this work.

Such decrease is faster for the sample 4060D, having the maximum of D enantiomer (15%) and becomes slower with decreasing D percentage. This is an indication that the amorphous chains are the first and more available for the hydrolytic attach from water molecules, as previously discussed with the acid based hydrolysis mechanism.

Reporting the glass transition temperature, Tg, evaluated by calorimetric analysis, as function of the reciprocal of Mn (Fig. 10), it is clear that the following relationship holds true [39]

$$\mathrm{Tg} = \mathrm{Tg}_{\infty} - \frac{K}{Mn} \tag{5}$$

namely a decrease of Mn is accompanied by a decrease of Tg [°C]. The value of the constant K, namely the slope of the plots reported in Fig. 10, is about the same for all the initially amorphous samples. The value of Tg_{∞} for amorphous samples increases with the amount of D isomer, consistently with what reported in the literature [40]. The initially crystalline sample departs from this behavior presenting a larger value of K, namely a larger dependence of Tg (°C) upon the molecular weight.

3.5. Description of hydrolysis by an autocatalytic mechanism

The carboxylic end-groups concentration, C_C, and the ester concentration, C_E, can be related to the molecular weight as follows [41]:

$$C_C = \frac{\rho}{M_n} \tag{6}$$

$$C_E = \frac{\rho}{M_n}(DP - 1) \tag{7}$$

In these equations ρ is the density of the polymer sample (about 1210 g/m^3) and DP is the average degree of polymerization, defined as the ratio M_n/M (M is the molecular weight of the repeating unit, equal to 72 g/mol in our case). Equation (6) takes into account the number of ester linkages in the monomer unit in the case of the polyesters studied in this work.

The kinetics of hydrolysis can be described by an autocatalytic mechanism [30]:

$$\frac{dC_C}{dt} = kC_CC_E \tag{8}$$

in which the kinetic constant k also includes the concentration of water inside the sample which can be assumed to be constant in the conditions adopted in this work.

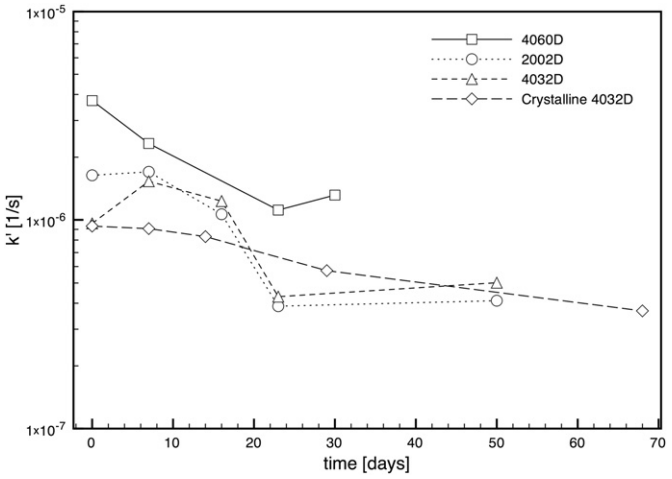

Fig. 11. Kinetic constant of the hydrolysis process.

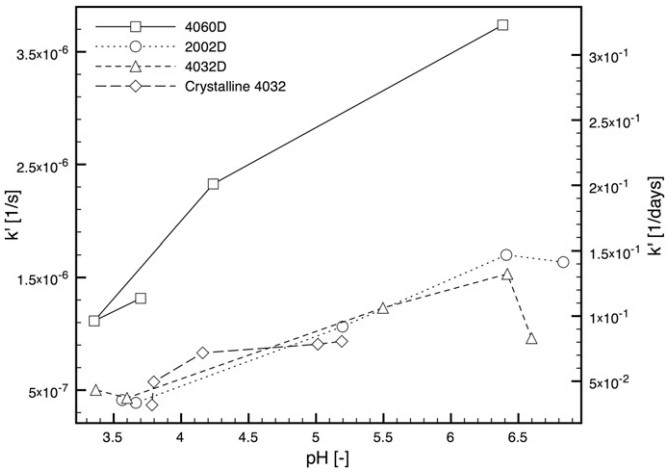

Fig. 12. Kinetic constant of the hydrolysis process versus the pH of the degrading medium.

After substituting Equations (6) and (7) into Eq. (8) and rearranging, also considering the definition of DP, Eq. (9) is obtained

$$\frac{dM_n}{dt} = -k\frac{\rho}{M}(M_n - M) \tag{9}$$

which can also be written as

$$\frac{d\ln(M_n - M)}{dt} = -k' \tag{10}$$

in which $k' = k\,\rho/M$ can be considered as the kinetic constant of the hydrolysis process.

The values that k' assumes during time can be calculated by knowing the time evolution of the number average molecular mass of the sample (reported in Fig. 9a) and is indeed nearly equal to the local slope of the plots reported in Fig. 9a, since M_n is always much larger than M. The results are reported in Fig. 11 and reveal that the kinetic constants tend to decrease with time for all the analyzed samples. It is worth mentioning that the order of magnitude of the constants are consistent with those found in the literature for the same temperature [12,42].

Although this change of the kinetic constant could raise doubts on the validity of the autocatalytic mechanism resulting in Eq. (10), it should be considered that the pH of the degrading medium changes upon time.

A plot of the kinetic constant of the hydrolysis process versus the pH of the degrading medium (reported in Fig. 12) reveals that k' depends linearly on pH and increases on increasing pH in the range 3.4–7 [43,44].

Following the results reported in Fig. 12 it appears that the degradation products of PLA induce changes in the pH of the degrading medium, which on its turn affects the kinetics of the degradation mechanism. No difference seems to hold between initially amorphous and initially crystalline samples as far as the effect of pH on the kinetic constant. 4060D presents a much higher kinetic constant and a higher dependence on pH [45]. Considering that all the other samples present different degrees of crystallinity and nevertheless behave in similar way, it appears that the D-lactide content can play a role in degradation kinetics apart from affecting the ability to crystallize of the samples.

4. Concluding remarks

This paper was focused on a detailed analysis of the hydrolysis process of three polylactic acid (PLA) grade samples with different

morphologies, obtained using different processing conditions. Such grades supplied by Natureworks, differing from D-isomer content, were named: 4060D (15% of D lactide) amorphous sample, 2002D (4% of D lactide) amorphous sample, 4032D (2% of D lactide) amorphous and semicrystalline samples. The hydrolysis process was monitored as function of time in bidistilled water at 58 °C using different techniques.

The conclusions can be summarized as follows:

- The monitoring of pH variation showed for amorphous samples an increasing of this parameter for the aqueous media in which the hydrolysis occurred, followed by a sharp decrease depending on the D content, suggesting an acid based hydrolysis mechanism. Semicrystalline sample did not show a pH increase during the first days of hydrolysis, but a quite constant value up 10 days, followed by a decreasing with lower rate compared to the amorphous one. Thus suggested the surface hydrolysis as the predominant phenomenon. All samples reached the same pH value after about 20 days of hydrolysis, independently of the microstructure and morphology of samples.
- The monitoring of crystallinity degree (*Xc%*), evaluated using DSC, WAXD and FTIR, showed that all the samples significantly increase their crystalline content during the hydrolysis tests. It was shown that at short times for all the samples some amorphous regions change into crystal, then the crystallinity degree increases by effect of the erosion of the amorphous parts. At long times also the crystalline regions undergo hydrolysis.
- GPC analysis showed that as consequence of hydrolytic process, the polymeric chains undergo a breakdown with a decreasing of Mw [Da] and Mn [Da] and also PDI. PDI index shows small variation with hydrolysis time. Such decreasing is faster for sample having the maximum of D enantiomer (15%) and becomes slower with decreasing D percentage. A good correlation holds between the glass transition temperature and the number average molecular weight of the samples
- The kinetics of hydrolysis was described by an autocatalytic mechanism and the evolution of molecular weight was adopted to calculate the kinetic constants for all the materials. It was found that the kinetic constants depend linearly on pH and increases on increasing pH in the range $3.4 \div 7$, suggesting that the degradation products of PLA induce changes in the pH of the degrading medium, which on its turn affects the kinetics of the degradation mechanism. No difference seems to hold between initially amorphous and initially crystalline samples as far as the effect of pH on the kinetic constant.
- The 4060D sample, having the largest D-lactide content, presented a much higher kinetic constant and a higher dependence on pH with respect to the other samples. Consistently, it also presented a faster weight loss. This phenomenon can be partly justified by the scarce ability of the sample to undergo crystallization, however the observed behavior seems to suggest that the D-lactide content can play a role itself, apart from crystallinity.

Acknowledgment

Thanks are due to Valentina Iozzino for carrying most of the experiments within her master thesis for degree in Chemical Engineering.

References

[1] Ikada Y, Tsuji H. Biodegradable polyesters for medical and ecological applications. Macromol Rapid Commun 2000;21:117–32.
[2] Lunt J. Large-scale production, properties and commercial applications of polylactic acid polymers. Polym Degrad Stabil 1998;59:145–52.
[3] Tsuji H, Daimon H, Fujie K. A new strategy for recycling and preparation of poly(L-lactic acid): hydrolysis in the melt. Biomacromolecules 2003;4:835–40.
[4] Saeki T, Tsukegi T, Tsuji H, Daimon H, Fujie K. Depolymerization of poly(L-lactic acid) under hydrothermal conditions. Kobunshi Ronbunshu 2004;61:561–6.
[5] Kopinke FD, Remmler M, Mackenzie K, Moder M, Wachsen O. Thermal decomposition of biodegradable polyesters .2. Poly(lactic acid). Polym Degrad Stabil 1996;53:329–42.
[6] Nishida H, Fan YJ, Mori T, Oyagi N, Shirai Y, Endo T. Feedstock recycling of flame-resisting poly(lactic acid)/aluminum hydroxide composite to L, L-lactide. Ind Eng Chem Res 2005;44:1433–7.
[7] Lostocco, Huang. The hydrolysis of poly(lactic acid) poly(hexamethylene succinate) blends. Polym Degrad Stabil 1998;61:225–30.
[8] Gonzalez MF, Ruseckaite RA, Cuadrado TR. Structural changes of polylactic-acid (PLA) microspheres under hydrolytic degradation. J Appl Polym Sci 1999;71:1223–30.
[9] Li SM, McCarthy S. Further investigations on the hydrolytic degradation of poly(DL-lactide). Biomaterials 1999;20:35–44.
[10] Tsuji H, Miyauchi S. Poly(L-lactide): 7. Enzymatic hydrolysis of free and restricted amorphous regions in poly(L-lactide) films with different crystallinities and a fixed crystalline thickness. Polymer 2001;42:4463–7.
[11] Tsuji H, Miyauchi S. Poly(L-lactide): VI Effects of crystallinity on enzymatic hydrolysis of poly(L-lactide) without free amorphous region. Polym Degrad Stabil 2001;71:415–24.
[12] Lyu, Schley J, Loy B, Lind D, Hobot ÄC. Kinetics and time-temperature equivalence of polymer degradation. Biomacromolecules 2007;8:2301–10.
[13] Zhang X, Espiritu M, Bilyk A, Kurniawan L. Morphological behaviour of poly(lactic acid) during hydrolytic degradation. Polym Degrad Stabil 2008;93:1964–70.
[14] Henton DE, Gruber P, Lunt J, Randall J. Polylactic acid technology. CRC Press LLC; 2005. p. 527–77.
[15] Hocking PJ, Timmins MR, Scherer TM, Fuller RC, Lenz RW, Marchessault RH. Enzymatic degradability of poly(beta-hydroxybutyrate) as a function of tacticity. J Macromol Sci Pure 1995;A32:889–94.
[16] Gogolewski S, Jovanovic M, Perren SM, Dillon JG, Hughes MK. Tissue-response and in-vivo degradation of selected polyhydroxyacids – polylactides (Pla), poly(3-hydroxybutyrate) (Phb), and poly(3-hydroxybutyrate-co-3-hydroxyvalerate) (Phb/Va). J Biomed Mater Res 1993;27:1135–48.
[17] Holland SJ, Jolly AM, Yasin M, Tighe BJ. Polymers for biodegradable medical devices .2. Hydroxybutyrate-hydroxyvalerate copolymers – hydrolytic degradation studies. Biomaterials 1987;8:289–95.
[18] Li SM, Garreau H, Vert M. Structure-property relationships in the case of the degradation of massive poly(alpha-hydroxy acids) in aqueous-media .3. Influence of the morphology of poly(L-lactic acid). J Mater Sci Mater M 1990;1:198–206.
[19] Li SM, Garreau H, Vert M. Structure property relationships in the case of the degradation of massive poly(alpha-hydroxy acids) in aqueous-media .2. Degradation of lactide-glycolide copolymers – Pla37.5ga25 and Pla75ga25. J Mater Sci Mater M 1990;1:131–9.
[20] Li SM, Garreau H, Vert M. Structure property relationships in the case of the degradation of massive aliphatic poly-(alpha-hydroxy acids) in aqueous-media .1. Poly(Dl-lactic acid). J Mater Sci Mater M 1990;1:123–30.
[21] Cheung HY, Lau KT, Lu TP, Hui D. A critical review on polymer-based bio-engineered materials for scaffold development. Compos Part B Eng 2007;38:291–300.
[22] Pantani R, Sorrentino A. Influence of crystallinity on the bio-degradation rate of injection molded poly(lactic acid) samples in controlled composting conditions. Polym Degrad Stabil 2013. http://dx.doi.org/10.1016/j.polymdegradstab.2013.01.005.
[23] Gilbert RD, Stannett V, Pitt CG, Schindler A. The design of biodegradable polymers: two approaches. Dev Polym Degrad 1982;4:259–93.
[24] Li SM. Hydrolytic degradation characteristics of aliphatic polyesters derived from lactic and glycolic acids. J Biomed Mater Res 1999;48:342–53.
[25] Tsuji H, Ikarashi K. In vitro hydrolysis of poly(L-lactide) crystalline residues as extended-chain crystallites. Part I: long-term hydrolysis in phosphate-buffered solution at 37 degrees C. Biomaterials 2004;25:5449–55.
[26] Höglund A, Odelius K, Albertsson AC. Crucial differences in the hydrolytic degradation between industrial polylactide and laboratory-scale poly(L-lactide). Appl Mater Interfaces 2012;4:2788–93.
[27] Höglund A, Hakkarainen M, Albertsson AC. Migration and hydrolysis of hydrophobic polylactide plasticizer. Biomacromolecules 2010;11:277–83.
[28] Pantani R, De Santis F, Sorrentino A, De Maio F, Titomanlio G. Crystallization kinetics of virgin and processed poly(lactic acid). Polym Degrad Stabil 2010;95:1148–59.
[29] De Santis F, Pantani R, Titomanlio G. Nucleation and crystallization kinetics of poly(lactic acid). Thermochim Acta 2011;522:128–34.
[30] Siparsky GL, Voorhees KJ, Miao FD. Hydrolysis of polylactic acid (PLA) and polycaprolactone (PCL) in aqueous acetonitrile solutions: autocatalysis. J Environ Polym Degr 1998;6:31–41.
[31] Vieira AC, Vieira JC, Ferra JM, Magalhaes FD, Guedes RM, Marques AT. Mechanical study of PLA-PCL fibers during in vitro degradation. J Mech Behav Biomed 2011;4:451–60.
[32] Sykes P. A guidebook to mechanism in organic chemistry. 4th ed. New York: Wiley; 1975.

[33] Furuhashi Y, Kimura Y, Yamane H. Higher order structural analysis of stereocomplex-type poly(lactic acid) melt-spun fibers. J Polym Sci Polym Phys 2007;45:218–28.
[34] Tsuji H, Takai H, Saha SK. Isothermal and non-isothermal crystallization behavior of poly(L-lactic acid): effects of stereocomplex as nucleating agent. Polymer 2006;47:3826–37.
[35] Partini M, Pantani R. Determination of crystallinity of an aliphatic polyester by FTIR spectroscopy. Polym Bull 2007;59:403–11.
[36] Krikorian V, Pochan DJ. Crystallization behavior of poly(L-lactic acid) nanocomposites: nucleation and growth probed by infrared spectroscopy. Macromolecules 2005;38:6520–7.
[37] Pan PJ, Yang JJ, Shan GR, Bao YZ, Weng ZX, Cao A, et al. Temperature-variable FTIR and solid-state C-13 NMR investigations on crystalline structure and molecular dynamics of polymorphic poly(L-lactide) and poly(L-lactide)/poly(D-lactide) stereocomplex. Macromolecules 2012;45:189–97.
[38] Fischer E, Sterzel H, Wegner G. Investigation of the structure of solution grown crystals of lactide copolymers by means of chemical reactions. Colloid Polym Sci 1973.
[39] Saeidlou S, Huneault MA, Li H, Park CB. Poly(lactic acid) crystallization. Prog Polym Sci 2012.
[40] Bigg DM. Polylactide copolymers: effect of copolymer ratio and end capping on their properties. Adv Polym Tech 2005;24:69–82.
[41] Partini M, Argenio O, Coccorullo I, Pantani R. Degradation kinetics and rheology of biodegradable polymers. J Thermal Anal Calorimetry 2009;98:645–53.
[42] Kolstad JJ, Vink ETH, De Wilde B, Debeer L. Assessment of anaerobic degradation of Ingeo (TM) polylactides under accelerated landfill conditions. Polym Degrad Stabil 2012;97:1131–41.
[43] De Jong S, Arias E, Rijkers D, Van Nostrum C, Kettenes-Van Den Bosch J, Hennink W. New insights into the hydrolytic degradation of poly (lactic acid): participation of the alcohol terminus. Polymer 2001;42:2795–802.
[44] Schliecker G, Schmidt C, Fuchs S, Kissel T. Characterization of a homologous series of D, L-lactic acid oligomers; a mechanistic study on the degradation kinetics in vitro. Biomaterials 2003;24:3835–44.
[45] Tsuji F. Autocatalytic hydrolysis of amorphous-made polylactides: effects of L-lactide content, tacticity, and enantiomeric polymer blending. Polymer 2002; 43:1789–96.